PCCP

Check for updates

Low-temperature FTIR spectroscopy of the L/Q switch of proteorhodopsin†

Tatsuro Nishikino,[ab] Teppei Sugimoto[a] and Hideki Kandori ⓘ *[ab]

Rhodopsins are photoreceptive membrane proteins containing a retinal chromophore, and the color tuning mechanism in rhodopsins is one of the important topics. Color switch is a color-determining residue at the same position, where replacement of red- and blue-shifting amino acids in two wild-type rhodopsins causes spectral blue- and red-shifts, respectively. The first and most famous color switch in microbial rhodopsins is the L/Q switch in proteorhodopsins (PRs). Green- or blue-absorbing PR (GPR or BPR) contains Leu and Gln at position 105 of the C-helix (TM3), respectively, and their replacement converted absorbing colors. The L/Q switch enables bacteria to absorb green or blue light in shallow or deep ocean waters, respectively. Although Gln and Leu are hydrophilic and hydrophobic residues, respectively, a comprehensive mutation study of position 105 in GPR revealed that the λ_{max} correlated with the volume of residues, not the hydropathy index. To gain structural insights into the mechanism, we applied low-temperature FTIR spectroscopy of L105Q GPR, and the obtained spectra were compared with those of GPR and BPR. The difference FTIR spectra of L105Q GPR were similar to those of BPR, not GPR, implying that the L/Q switch converts the GPR structure into a BPR structure in terms of the local environments of the retinal chromophore. It includes retinal skeletal vibration, hydrogen-bonding strength of the protonated Schiff base, amide-A vibration (peptide backbone), and protein-bound water molecules. Consequently color is switched accompanying such structural alterations, and known as the L/Q switch.

Rhodopsins are photoreceptive membrane proteins containing a retinal chromophore, which are classified into microbial and animal rhodopsins.[1–10] Microbial or animal rhodopsins contain either all-*trans* or 11-*cis* retinal, respectively, inside the seven transmembrane helices. The retinal chromophore is bound to a lysine residue of the seventh helix *via* a protonated Schiff base linkage. The color tuning mechanism is an important topic in the field of rhodopsins because the color of a common molecule, either the all-*trans* or 11-*cis* retinal Schiff base, is determined by the surrounding amino acid residues of the protein.[1–10] Color tuning is determined by various interactions between the retinal chromophore and protein, such as the electrostatic effect of charged groups, dipolar amino acid residues, aromatic amino acid residues, hydrogen-bonding interactions, and the steric contact effect.[11–19]

Although the mechanism is complex, it is well established that introduction of polar groups near the Schiff base or β-ionone ring stabilizes the electronically ground or excited state, respectively, leading to a spectral blue- or red-shift.[1] This is the case for the A/TS switch,[20–24] and the N/LI switch,[25] in microbial rhodopsins, where the color switch can be defined as a color-determining residue at the same position. Replacement of red- and blue-shifting amino acids in two wild-type rhodopsins causes spectral blue- and red-shifts, respectively. The position of the A/TS switch is one residue before retinal-binding Lys in the G-helix (TM7), located near the Schiff base, and the polar group causes spectral blue shift.[20–24] In contrast, the position of the N/LI switch is located near the β-ionone ring in the D-helix (TM4), and the polar group causes a spectral red shift.[25] However, the location of the color switch is very limited, as replacement of a residue surrounding the retinal chromophore easily destroys unique chromophore–protein interactions. Robustness is needed for the position of the color switch to maintain the chromophore–protein interactions.

Another famous color switch is the L/Q switch of proteorhodopsins (PRs).[26] Green- or blue-absorbing PR (GPR or BPR, Fig. S1, ESI†) contains Leu and Gln at position 105 of the C-helix (TM3), respectively,[27,28] and their replacement converted absorbing colors.[26] The L/Q switch was the first color switch discovered, and it is believed that bacteria absorb green or blue

a Department of Life Science and Applied Chemistry, Nagoya Institute of Technology, Showa-ku, Nagoya 466-8555, Japan. E-mail: kandori@nitech.ac.jp

b OptoBioTechnology Research Center, Nagoya Institute of Technology, Showa-ku, Nagoya 466-8555, Japan

This journal is © the Owner Societies 2024

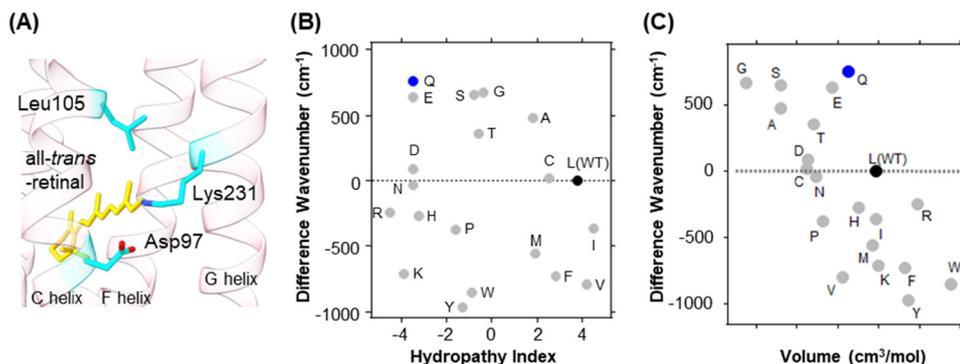*Phys. Chem. Chem. Phys.*, 2024, **26**, 22959–22967 | **22959**

Fig. 1 (A) Structure of the retinal chromophore and Leu105 in GPR (Protein Data Bank entry 7B03).[29] (B) Correlation between the absorption light energy of L105X GPR at pH 8 and the hydropathy index of the amino acid residue at position 105. The y-axis represents the difference in the wavenumber from that of the wild type (reciprocal λ_{max}; cm^{-1}), where positive and negative values correspond to the spectral blue- and red-shifts, respectively. The figure is modified from Ozaki et al.[31] (C) Correlation between the absorption light energy of L105X GPR at pH 8 and the volume of the amino acid residue at position 105. The y-axis represents the difference in the wavenumber from that of the wild type (reciprocal λ_{max}; cm^{-1}), where positive and negative values correspond to the spectral blue- and red-shifts, respectively. The figure is modified from Ozaki et al.[31]

light in shallow or deep ocean waters, respectively. The corresponding residue in a Haloarchaeal proton-pump bacteriorhodopsin (BR) is Leu93. In GPR and BPR, Leu and Gln are in direct contact with the 13-methyl group of the retinal chromophore (Fig. 1A), respectively.[29,30] Therefore, the L/Q switch for color tuning is presumably due to direct contact with the retinal chromophore.

As Gln and Leu are polar and non-polar residues, respectively, and position 105 is located near the Schiff base, it is reasonable to consider the color tuning mechanism of the L/Q switch owing to the introduction of a polar group into the Schiff base region. However, a previous comprehensive mutation study of position 105 in GPR revealed that absorption maxima did not correlate with the hydropathy index of residues (Fig. 1B).[31] In contrast, they correlate with the volume of the residues, though Gln and Leu possessed a similar volume (Fig. 1C). A positive correlation with volume, but not with hydropathy, suggests a complex mechanism of the L/Q switch. Previous solid-state NMR spectroscopy reported a detailed structural comparison between GPR and L105Q GPR.[32] In addition, the same group recently reported an integrated approach combining solid-state NMR spectroscopy and quantum mechanics/molecular mechanics (QM/MM) calculations of the L/Q switch of PRs, suggesting evolutionary robustness of the color switch.[33] On the other hand, the NMR study did not report on the analysis of BPR.

In this study, we applied light-induced difference FTIR spectroscopy to L105Q GPR at 77 K, which were compared with those of the wild-type GPR and BPR. The difference spectra at 77 K provide structural changes before and after retinal photoisomerization, including structural changes of the retinal chromophore and its binding pocket comprised of side-chains of protein, peptide backbone, and internal water molecules.[34] In addition to the conventional 1800–800 cm^{-1} region, frequencies at >1800 cm^{-1} provide O–H and N–H stretching modes (O–D and N–D in D$_2$O), which are the direct probe of hydrogen bonds.[35,36] In the spectra of a light-driven proton-pump bacteriorhodopsin (BR), we identified the obtained peaks by use of

[ς-^{15}N]lysine-labeled,[37,38] [η$_{1,2}$-^{15}N]arginine-labeled,[39] and [3-^{18}O]threonine-labeled[40–42] proteins in collaboration with the Herzfeld group. These vibrational bands as well as water O–D stretches in D$_2$O provided important information about hydrogen-bonding networks in BR. Since then, similar measurements were applied to other microbial rhodopsins,[34] including GPR.[43] The present comparative FTIR investigation of L105Q GPR with those of GPR and BPR revealed that the L-to-Q mutation of GPR switches various structural aspects from GPR-like into BPR-like, not only absorbing light wavelengths. The molecular mechanism of the mutation effect on the color switch will be discussed based on the present FTIR results.

Results

Difference UV-visible spectra of GPR, L105Q GPR, and BPR at 77 K

In the present study, each protein was expressed by *E. coli* cells, followed by purification and reconstitution into lipid membranes. In this study, all measurements were performed at pH 10, where the Schiff base counterion is negatively charged. Fig. S2 (ESI†) compares absorption spectra of hydrated films at pH 10 and 300 K, where GPR, L105Q GPR, and BPR exhibit λ_{max} values at 518 nm, 497 nm, and 490 nm, respectively. We then examined light-induced spectral changes in the UV-visible region at 77 K. To achieve this aim, each protein embedded in lipids was first dried and then rehydrated, as is standardly performed for various rhodopsins.[34,43,44]

Illumination of GPR at 510 nm caused spectral red-shift, whose difference spectrum exhibits the negative and positive peaks at 472 and 573 nm, respectively (red line in Fig. 2A). This indicates the formation of the K intermediate, as well as other microbial rhodopsins. Subsequent illumination at >560 nm showed complete photoreversion to the initial spectrum (black line in Fig. 2A), and the difference spectrum (dotted line in Fig. 1B) is a mirror image of the red line in Fig. 2A. We then
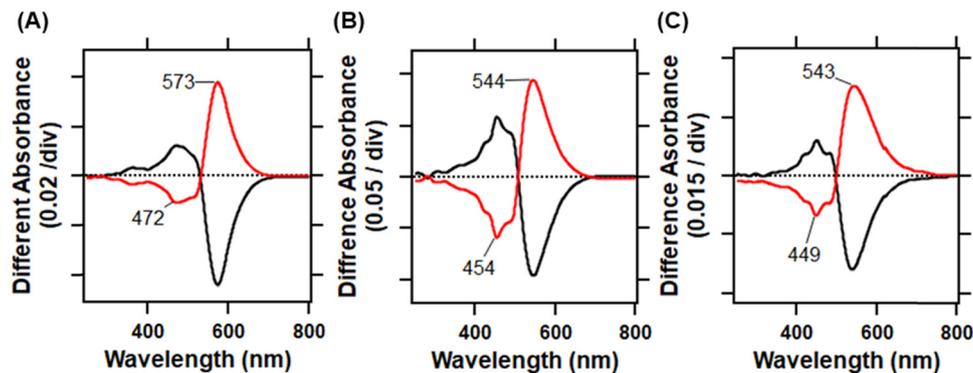
22960 | *Phys. Chem. Chem. Phys.*, 2024, **26**, 22959–22967

This journal is © the Owner Societies 2024

Fig. 2 Light-induced difference UV-visible spectra of GPR (A), L105Q GPR (B), and BPR (C) at pH 10 and 77 K. Red lines represent difference spectra by illumination at 510 nm (A), 470 nm (B), and 480 nm (C), which form the red-shifted K intermediate. Black lines represent difference spectra by subsequent illumination at >560 nm (A), >530 nm (B), and >530 nm (C), which revert to the original state. Mirror imaged spectral features indicate the two states being photoconvertible with each other.

illuminated L105Q GPR at 470 nm or BPR at 480 nm, and the produced K intermediates were reverted by subsequent illuminations at >530 nm. Fig. 2B and C for L105Q GPR and BPR, respectively, show mirror images like GPR (Fig. 2A), indicating photochromism between the unphotolyzed state and K intermediate.

Difference FTIR spectra of GPR, L105Q GPR, and BPR in the 1800–800 cm^{-1} region at 77 K

We next applied FTIR analysis under the same illumination conditions. Top panel of Fig. 3 shows such FTIR analysis of each protein at 77 K (for superimposed spectral comparison of L105Q GPR with those of GPR and BPR, see Fig. S3, ESI†). Positive and negative signals in the difference spectra originate from vibrational bands of the K intermediate and the initial state, respectively. The obtained difference spectra were compared among GPR, L105Q GPR, and BPR in H_2O (black line) and D_2O (red line). The low-frequency shift of the ethylenic stretching vibration (C=C stretch), at 1541(−)/1522(+) cm^{-1} in GPR, at 1550(−)/ 1524(+) cm^{-1} in L105Q GPR, and at 1552(−)/1528(+) cm^{-1} in BPR, is consistent with the formation of a red-shifted K intermediate (Fig. 3). Such a spectral feature is the most prominent in all PRs. In the C–C stretching region, all proteins exhibit a negative peak at ~1200 cm^{-1} and a positive peak at ~1194 cm^{-1} (Fig. 3), which is an indication of the conversion from the all-*trans* to the 13-*cis* form. On the other hand, peak frequencies of L105Q GPR (1202(−)/1194(+) cm^{-1}) are 2 cm^{-1} up-shifted from those of GPR (1200(−)/1192(+) cm^{-1}), and the same as those of BPR, suggesting a similar retinal structure of L105Q GPR to BPR, but not to GPR. Previous solid-state NMR study of GPR and L105Q GPR reported structural perturbation at the C14–C15 moiety of the retinal chromophore by mutation,[32] which is consistent with the present results.

Hydrogen out-of-plane (HOOP) vibrations appear at 1000– 900 cm^{-1}, where positive bands signify retinal distortion upon photoisomerization. When peaks are shifted between H_2O and D_2O, they are assignable for the HOOP vibrations near the Schiff base as the protonated Schiff base only differs between H_2O (C=NH) and D_2O (C=ND). Fig. 4 enlarges the HOOP
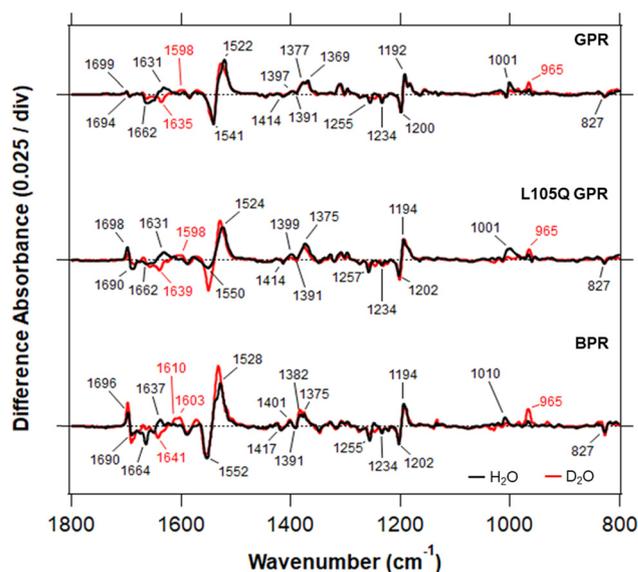

Fig. 3 Light-induced difference FTIR spectra of GPR, L105Q GPR, and BPR (from top to bottom) in the 1800–800 cm^{-1} region at pH 10 and 77 K. Positive and negative bands originate from vibrational bands of the K intermediate and initial state, respectively. Black and red lines are measured in H_2O and D_2O, respectively. The H_2O and D_2O spectra of GPR, L105Q GPR, and BPR are scaled by 0.88 and 1.00, 1.44 and 3.29, and 2.40 and 2.84, respectively.

region. In H_2O, the bands at 967(+)/960(−) cm^{-1} were observed in all spectra, while other bands differ with each other. The most intense peak appeared at 1001 cm^{-1} for GPR and 1010 cm^{-1} for BPR, whereas L105Q GPR shows a very broad band whose peak is located in between. This suggests the structure of the primary K intermediate of L105Q GPR is different from those of GPR and BPR. Similarly, a positive frequency at 1020 cm^{-1} in L105Q GPR is located between those of GPR (1018 cm^{-1}) and BPR (1022 cm^{-1}). On the other hand, a positive frequency at 1033 cm^{-1} in L105Q GPR is the same as that in BPR, not in GPR (1026 cm^{-1}). In D_2O, spectral similarity is noticeable as is seen for common positive bands at 984, 965,
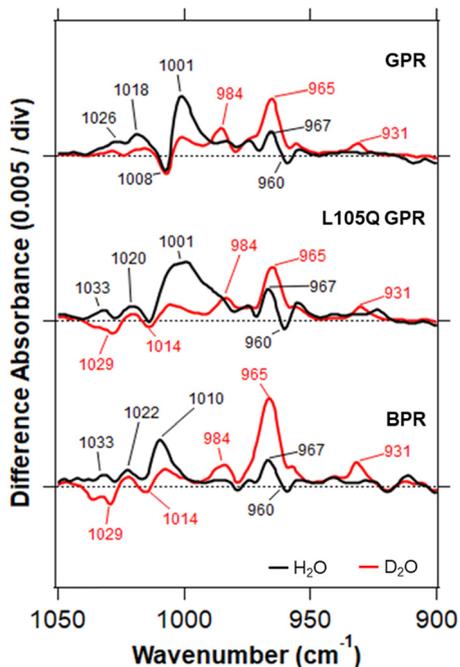
Fig. 4 Light-induced difference FTIR spectra of GPR, L105Q GPR, and BPR (from top to bottom) in the 1050–900 cm^{-1} region. Black and red lines are measured in H_2O and D_2O, respectively.

and 931 cm^{-1}. On the other hand, negative peaks at 1029 and 1014 cm^{-1} are common between L105Q GPR and BPR, but not GPR (Fig. 4).

Difference spectra in the 1760–1560 cm^{-1} region contain various protein vibrations including amide-I, the C=O stretch of the peptide backbone. The C=N stretching vibration of the protonated Schiff base only appears as the chromophore vibration in this region. The C=N stretching mode is coupled to the N–H bending vibration of the Schiff base, by which C=NH stretch is up-shifted from C=ND stretch. The difference in frequency between H_2O and D_2O has been regarded as a measure of hydrogen-bonding strength of the Schiff base.[45] Fig. 3 shows that the H/D exchangeable negative peaks appear at 1662 cm^{-1} in H_2O and at 1635 cm^{-1} in D_2O for GPR, at 1662 cm^{-1} in H_2O and at 1639 cm^{-1} in D_2O for L105Q GPR, and at 1664 cm^{-1} in H_2O and at 1641 cm^{-1} in D_2O for BPR. Consequently, the difference of L105Q GPR (23 cm^{-1}) is closer to that of BPR (23 cm^{-1}), not GPR (27 cm^{-1}). This suggests that the hydrogen bond of the Schiff base of GPR becomes BPR-like by a point mutation at position 105. Similar results were obtained by resonance Raman study.[46] The hydrogen bonding strength of the Schiff base will be discussed in more detail below, based on the data from its N–D stretching region.

Protonated carboxylic acids exhibit C=O stretches at 1800–1700 cm^{-1}, while COO$^-$ stretching vibrations of deprotonated species appear at 1600–1550 cm^{-1} (asymmetric mode) and 1430–1370 cm^{-1} (symmetric mode). In GPR and BPR, aspartates such as D97 and D227 act as the Schiff base counterion, and thus there are no bands at 1800–1700 cm^{-1} (Fig. 3). In contrast, peaks at 1440–1330 cm^{-1} presumably originate from

COO$^-$ stretch of D97 or D227. Previous mutation study of GPR revealed that these bands were preserved in D97N and D97E, but disappeared in D227N, from which the most straightforward interpretation is that the bands originate from the COO$^-$ stretch of D227.[43] Fig. 3 shows similar spectral features among GPR, L105Q GPR, and BPR, suggesting a similar local environment around D227.

Amide-I vibration, C=O stretch of the peptide backbone, appears at 1700–1600 cm^{-1}, which is a good probe of protein structural changes. As the C=N stretch of the Schiff base appears in the same frequency region, amide-I changes are unclear. We analyze peptide backbone changes from amide-A vibration, N–H stretch of the peptide backbone below. In contrast, the 1700–1680 cm^{-1} region is noteworthy, which is characteristic of C=O stretch of side-chains of asparagine and glutamine. In general, the C=O stretch exhibits small downshift upon deuteration of the side-chain (COND$_2$). Fig. 5 shows much larger spectral changes for L105Q GPR and BPR than those of GPR (for superimposed spectral comparison of L105Q GPR with those of GPR and BPR, see Fig. S4, ESI†). As the formers contain glutamine at position 105, straightforward interpretation is that the bands in L105Q GPR and BPR originate from the C=O stretch of Q105. The bands in GPR were coincident between H_2O and D_2O, suggesting that corresponding asparagine or glutamine is not deuterated in D_2O. It is also the case in BPR, though the positive peak looks slightly upshifted in D_2O. In contrast, a positive peak of L105Q GPR at 1698 cm^{-1} shifts to 1696 cm^{-1} in D_2O. From these observations, the side-chain of Q105 is not deuterated in BPR, but
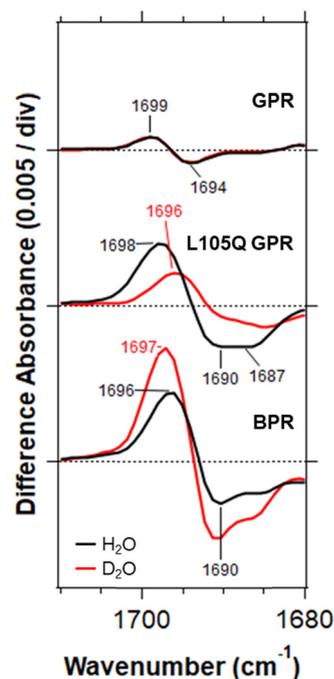

Fig. 5 Light-induced difference FTIR spectra of GPR, L105Q GPR, and BPR (from top to bottom) in the 1710–1680 cm^{-1} region. Black and red lines are measured in H_2O and D_2O, respectively.

22962 | *Phys. Chem. Chem. Phys.*, 2024, **26**, 22959–22967

This journal is © the Owner Societies 2024

deuterated in L105Q GPR, possibly because of the more flexible protein structure of the mutant.

Difference FTIR spectra of GPR, L105Q GPR, and BPR in the 2800–1800 cm^{-1} region upon hydration of D$_2$O at 77 K

Fig. 6 compares difference spectra in the 2800–1900 cm^{-1} region, which contains the X–D stretching vibrations of protein and water molecules. A spectral comparison of the samples hydrated with D$_2$O and D$_2$^{18}O identifies O–D stretching vibrations of water molecules changing their frequencies upon retinal photoisomerization.[34] The vibrational bands exhibiting isotope-induced downshifts can be assigned to the O–D stretching vibrations of water (labeled in green in Fig. 6). The frequency region in Fig. 6 also contains X–D stretching vibrations other than those of water molecules.

The N–D stretching vibration of the retinal Schiff base appears in this frequency region, and the bands at 2250–2170(+) cm^{-1}, and 2160–2000(−) cm^{-1} in GPR were identified as the N–D stretching vibrations of the retinal Schiff base by use ^{15}N Lys labeled GPR (Fig. 6).[43] The upshift by ∼70 cm^{-1} indicates that the hydrogen bond of the Schiff base in GPR is weakened upon formation of the *K* intermediate, which is however much smaller than in BR (upshift by >300 cm^{-1}).[37] Fig. 6 clearly shows no bands at <2100 cm^{-1} in L105Q GPR, which is also the case in BPR. These observations suggest that N–D stretching frequency of the Schiff base is higher in L105Q GPR and BPR than in GPR, indicating that the hydrogen bond of the Schiff base is weaker in L105Q GPR and BPR than in GPR. N–D stretches are possibly located at 2170–2171 cm^{-1} in L105Q GPR and BPR. These results are consistent with the analysis of the C=NH and C=ND vibrations (Fig. 3).

The green-labeled frequencies correspond to those identified as water stretching vibrations. In GPR, four negative peaks

at 2683, 2667, 2463, and 2315 cm^{-1} were earlier assigned to vibrations of water molecules, among which the frequency of the band at 2315 cm^{-1} is much lower than those of fully hydrated tetrahedral water molecules.[44] Comprehensive FTIR analysis of various rhodopsins revealed that proton-pumping rhodopsins contain strongly hydrogen-bonded water molecules, whose O–D stretch is located at <2400 cm^{-1} in D$_2$O.[34] Previous mutation study revealed that the water O–D stretches at 2530(+)/2385(+)/2315(−) cm^{-1} are influenced by the mutations of D97 and D227 in GPR.[43] It was thus concluded that these water molecules interact with the Schiff base counterion. Such a strongly hydrogen-bonded water molecule was similarly observed at 2384(+)/2362(−) cm^{-1} for L105Q GPR, and at 2402(+)/2328(−) cm^{-1} for BPR, together with a positive band at 2538 cm^{-1} for L105Q GPR and at 2557 cm^{-1} for BPR (Fig. 6). From the analogy with GPR, these water molecules can be assigned as the Schiff base water in L105Q GPR and BPR.

Previous study also showed that the water bands at 2683(−), 2676(+), 2667(−), 2634(+), 2482(+), and 2463(−) cm^{-1} were not influenced by the mutation of D97 and D227,[43] suggesting that such water molecules are not located in the vicinity of D97 and D227. Interestingly, both L105Q GPR and BPR show homologous bands at 2689(−)/2669(+) cm^{-1} and at 2689(−)/2674(+) cm^{-1}, respectively, to those at 2683(−)/2676(+) cm^{-1} in GPR, whereas corresponding other bands disappeared by a L-to-Q point mutation, which is also the case in BPR (Fig. 6). From these results, we infer that the water molecule(s) with the O–D stretches at 2667 and 2463 cm^{-1} are located in the vicinity of position 105. Upon photoisomerization, the O–D stretches shift to 2634 and 2482 cm^{-1}.

Difference FTIR spectra of GPR, L105Q GPR, and BPR in the 3650–3000 cm^{-1} region upon hydration of D$_2$O at 77 K

Fig. 7 compares difference spectra in the 3540–3000 cm^{-1} region in D$_2$O. As the frequency monitors X–H stretching vibrations that are not deuterated, O–H and N–H vibrations under hydrophobic conditions possibly appear. We can see spectral changes of H/D unexchangeable amide-A vibrations, N–H stretch of the peptide
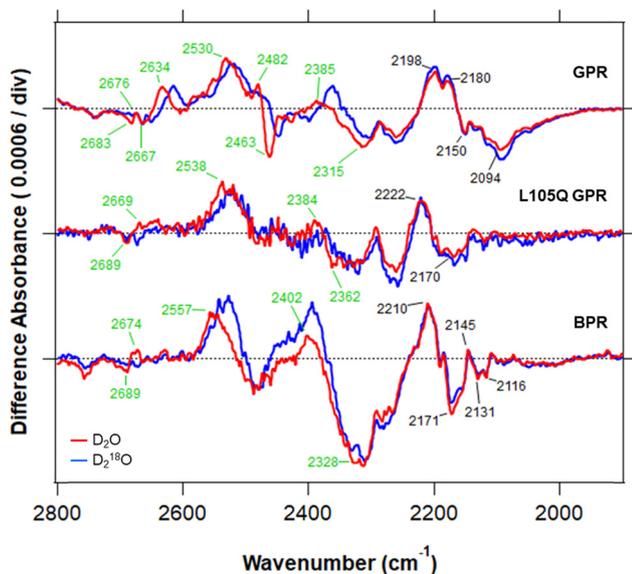

Fig. 6 Light-induced difference FTIR spectra of GPR, L105Q GPR, and BPR (from top to bottom) in the 2800–1900 cm^{-1} region at pH 10 and 77 K. Red and blue lines are measured in D$_2$O and D$_2$^{18}O, respectively. The D$_2$^{18}O spectra of GPR, L105Q GPR, and BPR are scaled by 1.11, 3.25 and 2.99, respectively.
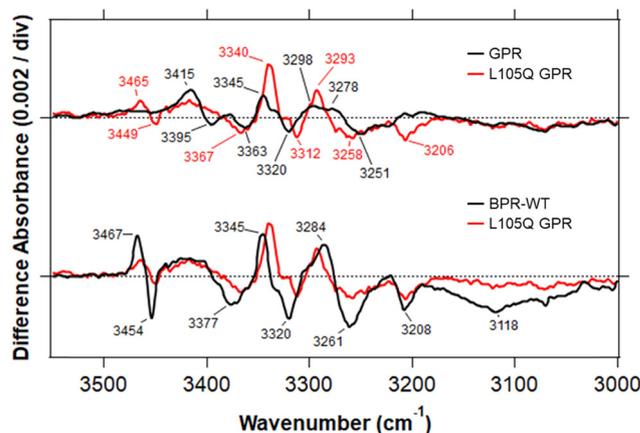

Fig. 7 Light-induced difference FTIR spectra of GPR (black line in the top panel), L105Q GPR (red lines), and BPR (black line in the bottom panel) in the 3540–3000 cm^{-1} region at pH 10 and 77 K, measured in D$_2$O.

backbone. Amide-A bands in GPR and BPR appear at 3345(+)/3320(−)/3298(+) cm^{-1} and at 3345(+)/3320(−)/3284(+) cm^{-1}, where spectral changes of BPR are more than twice larger than those of GPR. As is clearly seen in Fig. 7, amide-A changes in L105Q GPR are similar to those in BPR, not in GPR, indicating larger peptide backbone alterations than the wild-type GPR. This observation is intriguing, as mutation often suppresses normal structural changes of the protein. Nevertheless, in case of the L105Q mutation, GPR gains structural changes like BPR by a point mutation at position 105.

Another interesting observation was seen at > 3450 cm^{-1}. While there are no bands for GPR and a peak pair at 3467(+)/3454(−) cm^{-1} for BPR, In case of L105Q GPR, similar bands appeared at 3465(+)/3449(−) cm^{-1}. The straightforward interpretation is that the bands originate from N–H stretch of Q105, which is H/D unexchangeable. A smaller signal might be owing to the deuteration in L105Q GPR, and un-deuterated N–H stretch appeared. Another interpretation is that the bands at 3415(+)/3395(−) cm^{-1} in GPR is upshifted to 3465(+)/3449(−) cm^{-1} by the L-to-Q mutation.

Discussion

Amino acid identity is 79% between GPR and BPR (Fig. S1, ESI†). Therefore, two proteins possess highly homologous sequences, but ∼ 50 residues are still different from each other. Position 105 of GPR (position 106 in BPR; Fig. S1, ESI†) is well known as the L/Q switch, indicating that only the residue is responsible for color of PRs.[26] As Gln and Leu are polar and non-polar residues, respectively, the color tuning mechanism of the L/Q switch might be simply owing to the introduction of a polar group into the Schiff base region. However, previous comprehensive mutation study of position 105 in GPR provided unexpected results. Absorption light energy distributes randomly for 20 amino acids, when plotted *versus* their hydropathy index (Fig. 1B).[31] In contrast, absorption light energy correlates with the volume of the residues, where bulky amino acids cause spectral red shift (Fig. 1C).[31] Fig. 1C shows that glutamine deviates most significantly, suggesting a specific mechanism to exhibit blue-shift for L105Q.

This paper reports a comparative structural analysis by FTIR spectroscopy for GPR, L105Q GPR, and BPR, by which we are able to know that L105Q GPR is GPR-like or BPR-like structurally. To our surprise, the obtained difference FTIR spectra between the dark state and the primary K intermediate of L105Q GPR are more BPR-like than GPR-like, as seen in the C–C stretch of the retinal chromophore (Fig. 3), hydrogen-bonding strength of the protonated Schiff base (Fig. 3 and 6), amide-A vibration (peptide backbone) (Fig. 7), and protein-bound water molecules (Fig. 6). This suggests that an L-to-Q point mutation converted GPR into BPR structurally, which probably accompanies its color change. Below we discuss the structural mechanism of GPR, L105Q GPR, and BPR below.

Hydrogen-bonding strength of the protonated Schiff base

Hydrogen-bonding strength of the protonated Schiff base is experimentally monitored by vibrational spectroscopy or NMR spectroscopy. For the former, the difference between the C=NH and C=ND stretches is well established, where hydrogen bond is strong if the difference is large.[45,47–49] We also detected the N–D stretch of the Schiff base in D$_2$O, a more direct probe of hydrogen-bonding strength, where hydrogen bond is strong if the N–D stretch frequency is low.[37,43,50] For the latter, Herzfeld and her colleagues showed strong correlation with the ^{15}N chemical shift, where hydrogen bond is strong if the chemical shift is large.[51,52] Previous solid state NMR study observed identical chemical shifts between GPR and L105Q GPR, from which the same hydrogen-bonding strength was concluded.[32]

Unlike the previous solid-state NMR results, the present FTIR study clearly showed the hydrogen-bonding strength of the Schiff base switched from GPR-like to BPR-like by a point mutation at position 105. Such results were obtained by the analysis of (i) C=N stretch and (ii) N–D stretch in D$_2$O. The difference between C=NH and C=ND stretches in L105Q GPR (23 cm^{-1}) is close to that of BPR (23 cm^{-1}), not GPR (27 cm^{-1}) (Fig. 3), which is consistent with the previous results of the resonance Raman study.[46] A recent solid state NMR study reported different chemical shifts by 1 ppm between GPR and L105Q GPR,[33] which is also consistent with the present observations. N–D stretch in L105Q GPR (2170 cm^{-1}) is closer to that in BPR (2171 cm^{-1}) than in GPR (2094 cm^{-1}) (Fig. 6). Thus, hydrogen bonding strength of the protonated Schiff base is switched by the L-to-Q mutation of GPR. In general, strong interaction of the protonated Schiff base with its counterion localizes a positive charge at the Schiff base region, leading to a spectral blue-shift.[1,11–19] Strong hydrogen bond of the protonated Schiff base is normally coupled to such a strong interaction between the Schiff base and its counterion. Nevertheless, the hydrogen bond of the protonated Schiff base is stronger in the red-shifted GPR than in L105Q GPR and BPR, suggesting that other factors play a dominant role in color tuning.

Protein-bound water molecules

Regarding protein-bound water molecules, we observed 4 negative and 5 positive bands for GPR, 2 negative and 3 positive bands for L105Q GPR, and 2 negative and 3 positive bands for BPR (Fig. 6). These observations suggest that two pair bands of water in GPR disappeared in L105Q GPR, which may be also the case in BPR. Among these water molecules, water O–D stretches at 2530(+)/2385(+)/2315(−) cm^{-1} are influenced by the mutations of D97 and D227 in GPR,[43] and thus concluded to interact with the Schiff base counterion. These water bands were conserved in L105Q GPR and BPR. Therefore, water hydrogen bonds in the Schiff base region are similar among GPR, L105Q GPR, and BPR, though the Schiff base hydrogen bond is stronger in GPR than in L105Q GPR and BPR.

On the other hand, 3 negative and 3 positive bands for GPR were not influenced by the counterion mutations,[43] suggesting that these water molecules are located in other regions. As the water bands of GPR at 2667(−)/2634(+)/2482(+)/2463(−) cm^{-1} disappear in L105Q GPR, the straightforward interpretation is that these water molecules are located near L105 in GPR. Cryo-EM structure did not provide location of protein-bound water molecules because of limited resolution.[29] On the other hand,
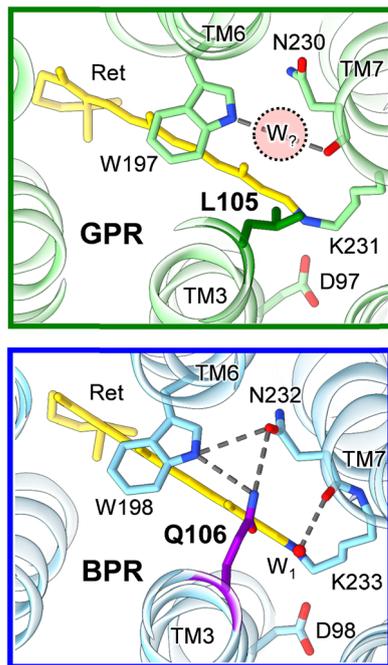
22964 | *Phys. Chem. Chem. Phys.*, 2024, **26**, 22959–22967

This journal is © the Owner Societies 2024

Fig. 8 Structural comparison of GPR (by cryo-EM, PDB: 7B03),[29] and BPR (by X-ray crystallography, PDB: 4JQ6),[30] viewed from the cytoplasmic side.

recent model structure based on the solid-state NMR and QM/MM calculations proposed the presence of a water molecule between W197 and N230 near L105 in GPR (top panel in Fig. 8), while the water is largely relocated in L105Q GPR.[33] Their proposal about the presence of a water molecule in GPR is consistent with our experimental results, though the crystal structure of BPR reported the presence of another water molecule near Q106 (W_1 in the bottom panel of Fig. 8).

Color-tuning mechanism

Previous mutation study of L105X GPR revealed the λ_{max} correlating with the volume of residues, not hydropathy index, though L and Q are similar in volume, but different in hydrophobicity (Fig. 1).[31] This suggests the presence of complex mechanisms for the L/Q switch, rather than a simple effect in hydrophobicity. The present comparative FTIR study clearly showed that the structure of L105Q GPR is more BPR-like, not GPR-like, despite the fact that a single residue was mutated among ∼50 different residues of GPR and BPR. It is thus likely that the L/Q switch switches the protein structure, and consequently absorbing color is also switched.

According to the GPR structure, L105 does not form interactions with F- and G-helices (TM6 and TM7, respectively) (Top Panel in Fig. 8).[29] In contrast, Q106 forms a hydrogen-bonding network with W198 and F-helix (TM6) and N232 in G-helix (TM7) (bottom panel in Fig. 8).[30] L105Q GPR presumably contains the similar hydrogen-bonding network, as proposed by the previous QM/MM calculation.[33] The present comparative FTIR study fully supports such a structural conversion, which includes a protein-bound water molecule. We suggest that the

L/Q switch works as the overall effect of the observed structural differences, which include retinal skeletal structure, hydrogen-bonding strength of the protonated Schiff base, peptide backbone, and protein-bound water molecules. It should be noted that the weaker hydrogen bond of the Schiff base in L105Q GPR than that in GPR plays an opposite effect to the spectral blue-shift, as described above. This suggests that other factors largely contribute to the spectral blue-shift in L105Q GPR and BPR. A highly polar hydrogen-bonding network containing Q105 in L105Q GPR and Q106 in BPR (bottom panel of Fig. 8) is probably one of the contributors.

It is noted that the volume dependence on absorbing colors in L105X GPR (Fig. 1) is still an open question. Previously we inferred the presence of two different mechanisms for large and small volumes.[31] The introduction of large amino acid residues into position 105 may disrupt the hydrogen-bonding network in the Schiff base region. This possibly weakens the interaction between the Schiff base and counterion (Asp97), leading to a spectral red-shift. In contrast, the introduction of small amino acid residues may cause penetrating of water molecules into the cavity. The resulting localization of a positive charge at the Schiff base would lead to a spectral blue-shift. The position of L105 in GPR (Q106 in BPR) is unique in microbial rhodopsins, whose roles in structure and function should be investigated.

Conclusions

Present difference FTIR spectroscopy of GPR and BPR at 77 K clearly demonstrated their own unique structures, which are derived from ∼50 different amino acid residues between them. The difference FTIR spectra of L105Q GPR were similar to those of BPR, not GPR, including retinal skeletal vibrations, vibrations of the protonated Schiff base, amide-A vibrations, and water stretching vibrations. This implies that the L/Q switch converts the GPR-like structure into BPR-like one in terms of the local environments of the retinal chromophore. The observed mutation-induced structural differences between GPR, L105Q GPR, and BPR are a prerequisite for the color switching effect. It should be noted that this is the study by the forward mutation of GPR, and full understanding of the mechanism will be gained by the reverse mutation of BPR, the Q-to-L mutant. In addition, structural alterations for other color switches, such as the A/TS switch,[20–24] G/P switch,[53,54] and N/LI switch,[25] is also intriguing. We reported structural differences in the chromophore vibrations for the A/TS and G/P switch mutants of a light-driven sodium-pump KR2 previously.[53] Comprehensive FTIR analysis will be our future focus.

Materials and methods

Sample preparation

To avoid the oxidation of cysteine residues in GPR, a triple-cysteine mutant (C107S/C156S/C175S) was used as a template for mutagenesis as described previously.[31,55] Additional L-to-Q mutation was introduced to design the L105Q GPR protein. On the other hand, we did not introduce cysteine mutations to

This journal is © the Owner Societies 2024

Phys. Chem. Chem. Phys., 2024, **26**, 22959–22967 | **22965**

prepare the BPR protein. C41 (DE3) cells carried the pET21a based plasmid corded GPR, L105Q GPR, and BPR with hexa-histidine tag in its C-terminal region were grown overnight in 10 ml of LB medium at 37 °C, inoculated in a 1.0 l of 2× TY medium (1.6% (w/v) tryptone, 1.0% (w/v) yeast extract and 0.5% (w/v) NaCl) and cultured at 37 °C. When the cell density at $OD_{660\ nm}$ approximately reached at 0.5, isopropyl β-D-thiogalactopyranoside (IPTG) and all-*trans* retinal was added to a final concentration of 1.0 mM and 10 μM, respectively, to induce the overexpression of PRs and cultured for 1 day at 37 °C. The cells were harvested by centrifugation and the weight of the cells was measured. 40 ml of A buffer (50 mM 2-(N-morpholino)ethanesulfonic acid (MES) [pH 6.5], 300 mM NaCl and 5 mM imidazole) were added and the cells were suspended. To break the cells, the suspension was treated twice by the French press at 100 MPa cm^{-2} (Ohtake). After unbroken cells were removed by low-speed centrifugation, the samples were ultra-centrifuged at $118\,000 \times g$ for 1 h. 40 ml of A buffer was added to suspend the resultant pellet and stored at −80 °C until use. The frozen sample was thawed and stirred in a water bath. To solubilize the suspension, DDM were added to a final concentration of 1% (w/v) and stirred for at least 60 min at 4 °C. Insoluble materials were removed by centrifugation ($120\,000 \times g$ for 30 min). The resultant supernatants were mixed with 30 ml of Talon Metal Affinity Resin (Takara) in a polypropylene column by the batch method. After eluting the supernatant in the column, 150 ml of B buffer (50 mM MES [pH 6.5], 300 mM NaCl, 50 mM imidazole, 0.1% (w/v) DDM) was added to wash the column. To elute His-tag protein from the resin, 40 ml of C buffer (50 mM Tris–HCl, pH 7.0, 300 mM NaCl, 300 mM imidazole, and 0.1% (w/v) DDM) was added and collected by 5 ml fractions. The fractions with its absorption ratio of λ_{525nm} to λ_{280nm} being 1 : 2–3 were mixed and concentrated to 3 ml using an Amicon device with 30 kDa cutoff (Merck Millipore). Then, concentrated sample dialysis with 200 ml of D buffer (20 mM 4-(2-hydroxyethyl)-1-piperazineethanesulfonic acid (PEPES) [pH 7.0], 100 mM NaCl, and 0.03% (w/v) DDM) twice to prepare for membrane reconstitution.

Low-temperature UV-visible and FTIR spectroscopy

Low-temperature UV-vis spectroscopy and FTIR spectroscopy were performed as described previously,[34–44] except for some minor modifications for reconstitution into the membrane. Briefly, the purified PR sample was reconstituted into POPE and POPG liposome, the molar ratio is 3 : 1, respectively, with a protein-to-lipid molar ratio of 1 : 50, and incubated for at least 1 hour at 4 °C. To remove the DDM micelles, Bio-Beads (SM-2, Bio-Rad) was added and incubated at 4 °C. The Bio-Beads in the lipid reconstruction solution was trapped using kitchen net. The sample in POPG-POPE liposomes was washed repeatedly with a buffer containing 1 mM NaCl and 2 mM N-cyclohexyl-3-aminopropanesulfonic acid (CAPS) (pH 10) and collected by ultracentrifugation for 20 minutes at $222\,000g$ at 4 °C. The lipid-reconstituted PRs was finally suspended in the same buffer and then placed on a BaF$_2$ window to prepare a dry-layer thin film. The films were hydrated with 1 μL H$_2$O, D$_2$O, or D$_2^{18}$O before

measurements. The sample was then placed in the cell of a cryostat (Optistat, Oxford Instruments) mounted in a UV-vis spectrometer (V-750, JASCO) and a FTIR spectrometer (Carry670, Agilent Technologies) and cooled to 77 K.

The GPR, L105Q GPR, and BPR samples were first illuminated with 510 nm, 470 nm, and 480 nm light (by the use of an interference filter) from a 1 kW halogen tungsten lamp at 77 K for 1 min, 4 min, and 1 min, respectively, converting PRs to an K intermediate. Then, the K intermediate of the GPR, L105Q GPR, and BPR were fully reconverted to its ground state upon illumination with >560 nm, >530 nm, and >530 nm light (O58, O55, and O55 filters) for 1 min, 2 min, and 1 min, which were evidenced by the spectral shape and amplitude in a mirror image of that for the ground state to K intermediate transition (Fig. 2). Therefore, we repeated cycles of alternating illumination with 510 nm and >560 nm lights for GPR, 470 nm and >530 nm lights for L105Q GPR, and 480 nm and >530 nm lights. We calculated the difference spectrum from the two spectra constructed from 128 interferograms taken before and after illumination. On average, 40, 64 and 65 deference spectra in the GPR, 64, 74 and 94 difference spectra in GPR-L105Q, and 44, 90 and 103 difference spectra in BPR obtained in this way, were used to produce the K intermediate of PRs minus ground state of PR spectra in the hydrated films of H$_2$O, D$_2$O, and D$_2^{18}$O, respectively.

Data availability

The data supporting this article have been included as part of the ESI.†

Conflicts of interest

The authors declare no competing financial interests.

Acknowledgements

References

1 O. P. Ernst, D. T. Lodowski, M. Elstner, P. Hegemann, L. S. Brown and H. Kandori, *Chem. Rev.*, 2014, **114**, 126–163.

2 M. Grote, M. Engelhard and P. Hegemann, *Biochim. Biophys. Acta.*, 2014, **1837**, 533–545.

3 L. S. Brown, *Biochim. Biophys. Acta.*, 2014, **1837**, 553–561.

4 E. G. Govorunova, O. A. Sineshchekov, H. Li and J. L. Spudich, *Annu. Rev. Biochem.*, 2017, **86**, 845–872.

22966 | *Phys. Chem. Chem. Phys.*, 2024, **26**, 22959–22967

This journal is © the Owner Societies 2024

5 A. N. Bondar and J. C. Smith, *Photochem. Photobiol.*, 2017, **93**, 1336–1344.

6 A. Rozenberg, K. Inoue, H. Kandori and O. Béjà, *Annu. Rev. Microbiol.*, 2021, **175**, 427–447.

7 V. Gordeliy, K. Kovalev, E. Bamberg, F. Rodriguez-Valera, E. Zinovev, D. Zabelskii, A. Alekseev, R. Rosselli, I. Gushchin and I. Okhrimenko, *Methods Mol. Biol.*, 2022, **2501**, 1–52.

8 K. Inoue, *J. Phys. Chem. B*, 2023, **127**, 9215–9222.

9 A. Terakita, *Genome Biol.*, 2005, **6**, 213.

10 K. Palczewski, *Annu. Rev. Biochem.*, 2006, **75**, 743–767.

11 P. E. Blatz, J. H. Mohler and H. V. Navangul, *Biochemistry*, 1972, **11**, 848–855.

12 R. Mathies and L. Stryer, *Proc. Natl. Acad. Sci. USA*, 1976, **73**, 2169–2173.

13 L. H. Andersen, I. B. Nielsen, M. B. Kristensen, M. O. A. El Ghazaly, S. Haacke, M. B. Nielsen and M. Å. Petersen, *J. Am. Chem. Soc.*, 2005, **127**, 12347–12350.

14 M. Hoffmann, M. Wanko, P. Strodel, P. H. König, T. Frauenheim, K. Schulten, W. Thiel, E. Tajkhorshid and M. Elstner, *J. Am. Chem. Soc.*, 2006, **128**, 10808–10818.

15 P. B. Coto, A. Strambi, N. Ferré and M. Olivucci, *Proc. Natl. Acad. Sci. USA*, 2006, **103**, 17154–17159.

16 S. Sekharan, M. Sugihara and V. Buss, *Angew. Chem., Int. Ed.*, 2007, **46**, 269–271.

17 S. Yokoyama, *Annu. Rev. Genomics Hum. Genet.*, 2008, **9**, 259–282.

18 G. Tomasello, G. Olaso-González, P. Altoè, M. Stenta, L. Serrano-Andrés, M. Merchán, G. Orlandi, A. Bottoni and M. Garavelli, *J. Am. Chem. Soc.*, 2009, **131**, 5172–5186.

19 K. Fujimoto, J. Hasegawa and H. Nakatsuji, *Bull. Chem. Soc. Jpn.*, 2009, **82**, 1140–1148.

20 K. Shimono, M. Iwamoto, M. Sumi and N. Kamo, *Photochem. Photobiol.*, 2000, **72**, 141–145.

21 K. Shimono, Y. Ikeura, Y. Sudo, M. Iwamoto and N. Kamo, *Biochim. Biophys. Acta, Biomembr.*, 2001, **1515**, 92–100.

22 K. Shimono, T. Hayashi, Y. Ikeura, Y. Sudo, M. Iwamoto and N. Kamo, *J. Biol. Chem.*, 2003, **278**, 23882–23889.

23 Y. Sudo, K. Ihara, S. Kobayashi, D. Suzuki, H. Irieda, T. Kikukawa, H. Kandori and M. Homma, *J. Biol. Chem.*, 2011, **286**, 5967–5976.

24 Y. Sudo, A. Okazaki, H. Ono, J. Yagasaki, S. Sugo, M. Kamiya, L. Reissig, K. Inoue, K. Ihara, H. Kandori, S. Takagi and S. Hayashi, *J. Biol. Chem.*, 2013, **288**, 20624–20632.

25 M. Sugiura, M. Singh, S. P. Tsunoda and H. Kandori, *Biochemistry*, 2023, **62**, 2013–2020.

26 D. Man, W. Wang, G. Sabehi, L. Aravind, A. F. Post, R. Massana, E. N. Spudich, J. L. Spudich and O. Béjà, *EMBO J.*, 2003, **22**, 1725–1731.

27 O. Béjà, L. Aravind, E. V. Koonin, M. T. Suzuki, A. Hadd, L. P. Nguyen, S. B. Jovanovich, C. M. Gates, R. A. Feldman, J. L. Spudich, E. N. Spudich and E. F. DeLong, *Science*, 2000, **289**, 1902–1906.

28 O. Béjà, E. N. Spudich, J. L. Spudich, M. Leclerc and E. F. DeLong, *Nature*, 2001, **411**, 786–789.

29 S. Hirschi, D. Kalbermatter, Z. Ucurum, T. Lemmin and D. Fotiadis, *Nat. Commun.*, 2021, **12**, 4107.

30 T. Ran, G. Ozorowski, Y. Gao, O. A. Sineshchekov, W. Wang, J. L. Spudich and H. Luecke, *Acta Crystallogr., Sect. D: Biol. Crystallogr.*, 2013, **69**, 1965–1980.

31 Y. Ozaki, T. Kawashima, R. Abe-Yoshizumi and H. Kandori, *Biochemistry*, 2014, **53**, 6032–6040.

32 J. Mao, N. N. Do, F. Scholz, L. Reggie, M. Mehler, A. Lakatos, Y. S. Ong, S. J. Ullrich, L. J. Brown and R. C. D. Brown, *et al.*, *J. Am. Chem. Soc.*, 2014, **136**, 17578–17590.

33 J. Mao, X. Jin, M. Shi, D. Heidenreich, L. J. Brown, R. C. D. Brown, M. Lelli, X. He and C. Glaubitz, *Sci. Adv.*, 2024, **10**, eadj0384.

34 H. Kandori, *Bull. Chem. Soc. Jpn.*, 2020, **93**, 904–926.

35 H. Kandori, N. Kinoshita, Y. Shichida and A. Maeda, *J. Phys. Chem. B*, 1998, **102**, 7899–7905.

36 H. Kandori and Y. Shichida, *J. Am. Chem. Soc.*, 2000, **122**, 11745–11746.

37 H. Kandori, M. Belenky and J. Herzfeld, *Biochemistry*, 2002, **41**, 6026–6031.

38 N. Mizuide, M. Shibata, N. Friedman, M. Sheves, M. Belenky, J. Herzfeld and H. Kandori, *Biochemistry*, 2006, **45**, 10674–10681.

39 T. Tanimoto, M. Shibata, M. Belenky, J. Herzfeld and H. Kandori, *Biochemistry*, 2004, **43**, 9439–9447.

40 H. Kandori, N. Kinoshita, Y. Yamazaki, A. Maeda, Y. Shichida, R. Needleman, J. K. Lanyi, M. Bizounok, J. Herzfeld, J. Raap and J. Lugtenburg, *Biochemistry*, 1999, **38**, 9676–9683.

41 H. Kandori, N. Kinoshita, Y. Yamazaki, A. Maeda, Y. Shichida, R. Needleman, J. K. Lanyi, M. Bizounok, J. Herzfeld, J. Raap and J. Lugtenburg, *Proc. Natl. Acad. Sci. USA*, 2000, **97**, 4643–4648.

42 H. Kandori, Y. Yamazaki, Y. Shichida, J. Raap, J. Lugtenburg, M. Belenky and J. Herzfeld, *Proc. Natl. Acad. Sci. USA*, 2001, **98**, 1571–1576.

43 D. Ikeda, Y. Furutani and H. Kandori, *Biochemistry*, 2007, **46**, 5365–5373.

44 Y. Furutani, D. Ikeda, M. Shibata and H. Kandori, *Chem. Phys.*, 2006, **324**, 705–708.

45 T. Baasov, N. Friedman and M. Sheves, *Biochemistry*, 1987, **26**, 3210–3217.

46 J. M. Kralj, E. N. Spudich, J. L. Spudich and K. J. Rothscild, *J. Phys. Chem. B*, 2008, **112**, 11770–11776.

47 A. Lewis, J. Spoonhower, R. A. Bogomolni, R. H. Lozier and W. Stoeckenius, *Proc. Natl. Acad. Sci. USA*, 1974, **71**, 4462–4466.

48 B. Aton, A. G. Doukas, R. H. Callender, B. Becher and T. G. Ebrey, *Biochemistry*, 1977, **16**, 2995–2999.

49 M. Braiman and R. Mathies, *Biochemistry*, 1980, **19**, 5421–5428.

50 M. Shibata, N. Muneda, T. Sasaki, K. Shimono, N. Kamo, M. Demura and H. Kandori, *Biochemistry*, 2005, **44**, 12279–12286.

51 G. S. Harbison, J. Herzfeld and R. G. Griffin, *Biochemistry*, 1983, **22**, 1–4.

52 H. J. de Groot, G. S. Harbison, J. Herzfeld and R. G. Griffin, *Biochemistry*, 1989, **28**, 3346–3353.

53 K. Inoue, M. del Carmen Marín, S. Tomida, R. Nakamura, Y. Nakajima, M. Olivucci and H. Kandori, *Nat. Commun.*, 2019, **10**, 1993.

54 Y. Nakajima, L. Pedraza-González, L. Barneschi, K. Inoue, M. Olivucci and H. Kandori, *Commun. Biol.*, 2021, **4**, 1185.

55 R. A. Krebs, U. Alexiev, R. Partha, A. M. DeVita and M. S. Braiman, *BMC Physiol.*, 2002, **2**, 5.

This journal is © the Owner Societies 2024

Phys. Chem. Chem. Phys., 2024, **26**, 22959–22967 | **22967**